11th International Symposium on Practical Design of Ships and Other Floating Structures
Rio de Janeiro, RJ, Brazil

Maneuvering of Two Interacting Ships in Calm Water

Xu Xiang [1], Odd M. Faltinsen [1) 2)]

[1)] Center for Ships and Ocean Structures (CeSOS), Norwegian University of Science and Technology
Trondheim, Norway

[2)] Department of Marine Technology, Norwegian University of Science and Technology
Trondheim, Norway

Abstract

The maneuvering of two interacting ships in calm water at Froude numbers less than ~0.2 and in water of infinite horizontal extent is studied based on an extended version of the maneuvering model for two ships by Skejic (2008). The time-varying interacting forces/moments and maneuvering hydrodynamic derivatives are obtained via a new method assuming 3D potential flow with a rigid-free-surface condition around non-lifting bodies. The two bodies can have any relative positions and move with any velocities in the horizontal plane. The method is verified and validated. The model is applied to an overtaking maneuver that was studied by Skejic (2008) documenting that it matters with the improved hydrodynamic interaction model.

Keywords

Maneuverability, hydrodynamic interaction, overtaking maneuver, auto-pilot

Introduction

Maneuvering of two ships is important for both civic and naval applications. Transfer of cargos or oil at sea, offshore operations, underway replenishment of naval fleets and canal transportation all involve such maneuver. Previous study on this problem can be found in, for example, Alvestad and Brown (1975), Yasukawa (2003), Skejic (2008), Skejic and Faltinsen (2008) and Skejic et al. (2009). The hydrodynamic interaction loads between the two vessels play an important role. This paper focuses on maneuvering of two ships in calm water. Except for recent computational fluid dynamics (CFD) applications (Cheng, 2006), the hydrodynamic problem is mainly studied based on a potential flow assumption. Relevant interaction models between two bodies can be divided into two main classes: theoretical study based on slender body theories (Newman, 1965; Tuck and Newman, 1974; Skejic, 2008; Wang, 2007, etc.) and numerical solutions based on boundary element method (BEM) (Korsmeyer et al. 1996; Pinkster, 2004; Cheng, 2007). The presented maneuvering model has a new formulation of the interacting yaw moment and horizontal force acting on two ships with different time-dependent horizontal velocities and yaw angles. The assumption is 3D potential flow without wave effects around non-lifting bodies. Body-fixed coordinate systems are used. A BEM with source distributions over the two interacting bodies is used to determine the time-dependent flow velocity. Because there are no limitations regarding how close the ships can be, we may simulate up to the time of collision.

Maneuvering model of two interacting ships in calm water

The two ships are named Ship *I (I=1,2)*. The body-fixed coordinate systems for the two ships are denoted $O_I x_I y_I z_I$ where the origin O_I coincides with the center of gravity (CoG) of the ship (see Fig. 1). Positive z_I is upwards. The $O_I x_I z_I -$ plane includes

the ship's center plane and positive x_1 is forwards. u_1 and u_2 denote the longitudinal and lateral components of the velocity of ship 1. u_3 is the yaw angular velocity of ship 1. u_4 and u_5 mean the longitudinal and lateral components of the velocity of ship 2. u_6 is the yaw angular velocity of ship 2. The Froude numbers *Fn* of the two ships are assumed sufficiently small, i. e. lower than ~0.2, in order for the steady wave generation to be secondary and a rigid free-surface condition can be assumed in a potential-flow formulation. Ishiguro et al. (1993) presented hydrodynamic maneuvering coefficients for the high-speed vessel "Super Slender Twin Hull" by means of planar motion mechanism (PMM) tests for *Fn≥0.184* showing that Froude number, i.e. steady wave generation matters. There are no external wave, current and wind acting on the ships. Our application and detailed discussion is for water of infinite depth and a free surface of infinite horizontal extent. However, the general expressions are the same for finite depth.

The equations of motions of the two ships formulated in the body-fixed accelerated coordinate system of each ship can formally be expressed as

$$\begin{aligned} M^{(1)}\left(\dot{u}_1 - u_3 u_2\right) &= X^{(1)}; M^{(1)}\left(\dot{u}_2 + u_3 u_1\right) = Y^{(1)}; I_{66}^{(1)}\dot{u}_3 = N^{(1)} \\ M^{(2)}\left(\dot{u}_4 - u_6 u_5\right) &= X^{(2)}; M^{(2)}\left(\dot{u}_5 + u_6 u_4\right) = Y^{(2)}; I_{66}^{(2)}\dot{u}_6 = N^{(2)} \end{aligned} \quad (1)$$

Here $M^{(I)}$ is the mass of ship *I* and $I_{66}^{(I)}$ is the mass moment of inertia in yaw relative to CoG of ship number *I*. $X^{(I)}$, $Y^{(I)}$,$N^{(I)}$ are the longitudinal force, transverse force and yaw moment with respect to CoG of ship number *I*. The forces and moments are composed of hydrodynamic terms associated with the hull, rudder and propulsion that will be separately discussed.

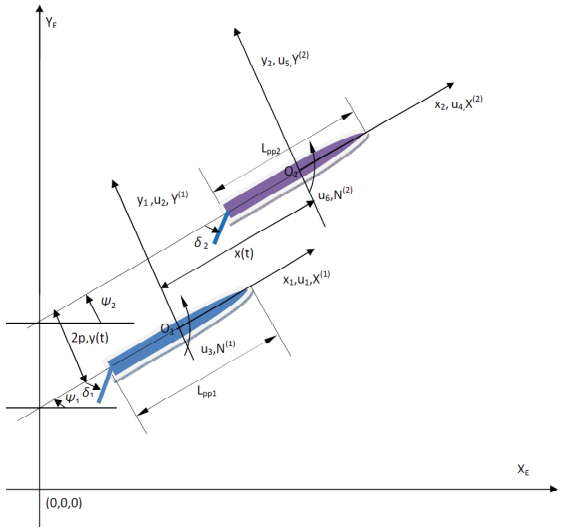

Fig. 1: Coordinate systems and notations used in maneuvering models for two interacting ships in calm water

Non-viscous and non-lifting hull loads

We start with the non-viscous and non-lifting hull loads and consider later separately lifting and viscous loads on the hulls. The load expressions must account for the fact that we operate with body-fixed coordinate systems. The potential flow around the ships is the same as the flow around the double-bodies of the ships in infinite fluid. The latter fact is due to the free-surface condition and the fact that we only consider horizontal ship motions. The x_1 – and y_1 – components of the non-lifting hydrodynamic force on ship number *I* can according to potential flow theory of incompressible water be expressed as

$$\begin{aligned} \mathbf{F}^{(I)} = \left(X_{NLH}^{(I)}, Y_{NLH}^{(I)}, 0\right) = -\frac{d}{dt}\left(\rho \iint_{S_H^{(I)}} \varphi \mathbf{n}^{(I)} dS\right) \\ -\rho \iint_{S_H^{(I)}} \left(0.5\mathbf{V}\cdot\mathbf{V}\mathbf{n}^{(I)} - \mathbf{V}V_n\right) dS \end{aligned} \quad (2)$$

The formula follows e.g. by using conservation of fluid momentum, vector algebra and generalized Gauss theorem and is consistent with the expression by Newman (1977). The subscript *NLH* in the notation for the longitudinal and transverse force components $X_{NLH}^{(I)}$ and $Y_{NLH}^{(I)}$ indicates "non-lifting hull". Further, $S_H^{(I)}$ is the wetted hull surface of ship number *I*, $\mathbf{n}^{(I)} = \left(n_x^{(I)}, n_y^{(I)}, n_z^{(I)}\right)$ is the normal vector

to $S_H^{(I)}$ with positive direction out of the water, ρ is the mass density of water, φ is the velocity potential of the flow, $\mathbf{V} = \nabla\varphi$ is the flow velocity and V_n is the normal component of $\mathbf{V}$ on $S_H^{(I)}$. The formula accounts for the interaction between the two ships through the velocity potential φ. Because we operate with accelerated coordinate systems, care must be shown in how the time differentiation in eq. (2) is performed. We define

$$\mathbf{B}^{(I)} = B_1^{(I)}\mathbf{e}_x^{(I)} + B_2^{(I)}\mathbf{e}_y^{(I)} = \rho\iint_{S_H^{(I)}}\varphi\begin{pmatrix} n_x^{(I)} \\ n_y^{(I)} \end{pmatrix} dS \tag{3}$$

Here $\mathbf{e}_x^{(I)}$ and $\mathbf{e}_y^{(I)}$ are unit vectors along the x_I- and y_I- axis, respectively. Because the unit vectors are time-dependent, it follows that

$$\frac{d\mathbf{B}^{(I)}}{dt} = \left(\frac{dB_1^{(I)}}{dt} - r^{(I)}B_2^{(I)}\right)\mathbf{e}_x^{(I)} + \left(\frac{dB_2^{(I)}}{dt} + r^{(I)}B_1^{(I)}\right)\mathbf{e}_y^{(I)} \tag{4}$$

with $r^{(1)} = u_3, r^{(2)} = u_6$. We define

$$n_1 = n_x^{(1)}, n_2 = n_y^{(1)}, n_3 = x^{(1)}n_2 - y^{(1)}n_1$$
$$n_4 = n_x^{(2)}, n_5 = n_y^{(2)}, n_6 = x^{(2)}n_5 - y^{(2)}n_4$$

where the coordinates $x^{(I)}$, $y^{(I)}$ are on the wetted hull surface. The velocity potential is expressed as

$$\varphi(x,y,z,t) = \sum_{i=1}^{6} u_i(t)\varphi_i(x,y,z,t) \tag{5}$$

Here φ_i satisfies the rigid free-surface condition and the following body-boundary conditions

$$\frac{\partial\varphi_i}{\partial n} = n_i \text{ on } S_H^{(1)}, \quad \frac{\partial\varphi_i}{\partial n} = 0 \text{ on } S_H^{(2)} \text{ when } i \le 3$$
$$\frac{\partial\varphi_i}{\partial n} = 0 \text{ on } S_H^{(1)}, \quad \frac{\partial\varphi_i}{\partial n} = n_i \text{ on } S_H^{(2)} \text{ when } i \ge 4$$

Further $\nabla\varphi_i \to 0$ at infinity. The boundary-value problems are in our case solved by distributing sources satisfying the rigid free-surface condition over the two body surfaces. This leads to determination of the added mass coefficients

$$A_{ij} = \rho\iint_{S_H^{(I)}}\varphi_j n_i dS \tag{6}$$

where *I=1* for *i=1,2,3* and *I=2* for *i=4,5,6*. It follows from eq. (3) and eq. (6) that

$$B_1^{(1)} = \sum_{j=1}^{6} A_{1j}u_j, B_2^{(1)} = \sum_{j=1}^{6} A_{2j}u_j,$$
$$B_1^{(2)} = \sum_{j=1}^{6} A_{4j}u_j, B_2^{(2)} = \sum_{j=1}^{6} A_{5j}u_j \tag{7}$$

Eq. (4) can be expressed in terms of A_{ij} and u_i which enables us to express the time derivative term in eq.(2). Further, we can use eq. (5) to find the flow velocity $\mathbf{V} = \nabla\varphi$ needed in eq. (2). It means that the force components $X_{NLH}^{(1)}$ and $Y_{NLH}^{(1)}$ along the x_1- and y_1- axis on ship 1 are

$$X_{NLH}^{(1)} = -\frac{d}{dt}\left(\sum_{j=1}^{6} A_{1j}u_j\right) + u_3\sum_{j=1}^{6} A_{2j}u_j - \rho\iint_{S_H^{(1)}}\left(0.5\mathbf{V}\cdot\mathbf{V}n_1 - V_1V_n\right)dS \tag{8}$$

$$Y_{NLH}^{(1)} = -\frac{d}{dt}\left(\sum_{j=1}^{6} A_{2j}u_j\right) - u_3\sum_{j=1}^{6} A_{1j}u_j - \rho\iint_{S_H^{(1)}}\left(0.5\mathbf{V}\cdot\mathbf{V}n_2 - V_2V_n\right)dS \tag{9}$$

where $\mathbf{V} = (V_1, V_2, V_3)$. The force components $X_{NLH}^{(2)}$ and $Y_{NLH}^{(2)}$ along the x_2- and y_2- axis on ship 2 are

$$X_{NLH}^{(2)} = -\frac{d}{dt}\left(\sum_{j=1}^{6} A_{4j}u_j\right) + u_6\sum_{j=1}^{6} A_{5j}u_j - \rho\iint_{S_H^{(2)}}\left(0.5\mathbf{V}\cdot\mathbf{V}n_4 - V_1V_n\right)dS \tag{10}$$

$$Y_{NLH}^{(2)} = -\frac{d}{dt}\left(\sum_{j=1}^{6} A_{5j}u_j\right) - u_6\sum_{j=1}^{6} A_{4j}u_j - \rho\iint_{S_H^{(2)}}\left(0.5\mathbf{V}\cdot\mathbf{V}n_5 - V_2V_n\right)dS \tag{11}$$

If the two vessels have a steady configuration relative to each other, have constant translatory velocities

and no yaw velocities, the interaction forces between the two vessels are expressed by the wetted surface integrals.

The hydrodynamic yaw moment with respect to CoG of ship *I* is the z_I-component of

$$\mathbf{L}^{(I)} = -\mathbf{u}_0^{(I)} \times \left(\rho \iint_{S_H^{(I)}} \mathbf{n}^{(I)} \varphi dS \right) - \frac{d}{dt}\left(\rho \iint_{S_H^{(I)}} \mathbf{r}_I \times \mathbf{n}^{(I)} \varphi dS \right) - \rho \iint_{S_H^{(I)}} \mathbf{r}_I \times \left(0.5\mathbf{V} \cdot \mathbf{V}\mathbf{n}^{(I)} - \mathbf{V} V_n \right) dS \quad (12)$$

Here $\mathbf{r}_I = x_I \mathbf{e}_x^{(I)} + y_I \mathbf{e}_y^{(I)} + z_I \mathbf{e}_z^{(I)}$ is the radius vector of points on the wetted hull surface relative to CoG and $\mathbf{u}_0^{(1)} = u_1 \mathbf{e}_x^{(1)} + u_2 \mathbf{e}_y^{(1)}, \mathbf{u}_0^{(2)} = u_4 \mathbf{e}_x^{(2)} + u_5 \mathbf{e}_y^{(2)}$ are the translatory velocities of the CoG of the ships. The formula follows e.g. by using conservation of angular fluid momentum, vector algebra and generalized Gauss theorem. The expression is consistent with Newman (1977) and Kochin et al. (1964). However, it differs from Newman (1977) because we consider the moment with respect to CoG. The consequence is the first term appearing on the right hand side of eq. (12). Further, the last integral on the right hand side of eq. (12) is expressed in Newman (1977) over a control surface instead over the hull surface. It follows by vector algebra and the generalized Gauss theorem that the expressions are the same. The expression differs from Kochin et al. (1964) because they considered a single body which implies that the last integral on the right hand side of eq. (12) disappears. Otherwise, the expression is the same.

The non-lifting yaw moment on the hull of ship number 1 can then be expressed as

$$N_{NLH}^{(1)} = u_2 \sum_{j=1}^{6} A_{1j} u_j - u_1 \sum_{j=1}^{6} A_{2j} u_j - \frac{d}{dt}\left(\sum_{j=1}^{6} A_{3j} u_j \right) - \rho \iint_{S_H^{(1)}} \left[n_3 0.5 V \cdot V - \left(x_1 V_2 - y_1 V_1 \right) \right] dS \quad (13)$$

The terms $u_2 \sum_{j=1}^{6} A_{1j} u_j - u_1 \sum_{j=1}^{6} A_{2j} u_j$ in eq. (13) include $\left(A_{11} - A_{22} \right) u_1 u_2$ which for a single ship without any interaction effects with other ships are referred to as the Munk moment. The non-lifting yaw moment on the hull of ship number 2 is

$$N_{NLH}^{(2)} = u_5 \sum_{j=1}^{6} A_{4j} u_j - u_4 \sum_{j=1}^{6} A_{5j} u_j - \frac{d}{dt}\left(\sum_{j=1}^{6} A_{6j} u_j \right) - \rho \iint_{S_H^{(2)}} \left[n_6 0.5 \mathbf{V} \cdot \mathbf{V} - \left(x_2 V_2 - y_2 V_1 \right) \right] dS \quad (14)$$

Eq.(2) and eq. (12) may by means of vector algebra and the generalized Gauss theorem be expressed as

$$\mathbf{F}^{(I)} = \left(X_{NLH}^{(I)}, Y_{NLH}^{(I)}, 0 \right) = -\frac{d}{dt}\left(\rho \iint_{S_H^{(I)}} \varphi \mathbf{n}^{(I)} dS \right) + \rho \iint_{S_C^{(I)}} \left(0.5\mathbf{V} \cdot \mathbf{V}\mathbf{n}^{(I)} - \mathbf{V} V_n \right) dS$$

$$\mathbf{L}^{(I)} = -\mathbf{u}_0^{(I)} \times \left(\rho \iint_{S_H^{(I)}} \mathbf{n}^{(I)} \varphi dS \right) - \frac{d}{dt}\left(\rho \iint_{S_H^{(I)}} \mathbf{r}_I \times \mathbf{n}^{(I)} \varphi dS \right) + \rho \iint_{S_C^{(I)}} \mathbf{r}_I \times \left(0.5\mathbf{V} \cdot \mathbf{V}\mathbf{n}^{(I)} - \mathbf{V} V_n \right) dS \quad (15)$$

where the closed control surfaces $S_C^{(I)}$ for body *I* is in the water and do not surround the other body. Positive direction of $\mathbf{n}^{(I)}$ on $S_C^{(I)}$ is out of the control volume. We have in our calculations used the originally presented formulas. However, it may be an advantage from a numerical accuracy point of view to avoid calculating the flow velocity at the body surface.

Hull lift force and moment

The lifting force component $Y_{LH}^{(I)}$ along the y_I-axis and yaw moment $N_{LH}^{(I)}$ on each hull will be analyzed by linear slender-body theory and by neglecting the hull interaction. It follows then (see e.g. Newman, 1977; Faltinsen, 2005) that

$$Y_{LH}^{(1)} = -a_{22T}^{(1)} u_1 u_2 - x_1^{(T)} a_{22T}^{(1)} u_1 u_3; \; Y_{LH}^{(2)} = -a_{22T}^{(2)} u_4 u_5 - x_2^{(T)} a_{22T}^{(2)} u_4 u_6$$
$$N_{LH}^{(1)} = -x_1^{(T)} a_{22T}^{(1)} u_1 u_2 - \left[x_1^{(T)} \right]^2 a_{22T}^{(1)} u_1 u_3;$$
$$N_{LH}^{(2)} = -x_2^{(T)} a_{22T}^{(2)} u_4 u_5 - \left[x_2^{(T)} \right]^2 a_{22T}^{(2)} u_4 u_6 \quad (16)$$

Here $x_I^{(T)}$ refers to the x_I-coordinate of the transom stern of ship I and $a_{22T}^{(I)}$ means the two-dimensional sway added mass at the transom. Formulas for $a_{22T}^{(I)}$ in deep water based on Lewis form technique can, for instance, be found in Faltinsen (2005). The terms in eq. (16) are physically associated with the fact that the flow separates from the transom and leave a vortex sheet downstream from the transom in the

$O_I x_I z_I$ – plane. Søding (1982) suggests modifying the formula in case of non-slender ships by setting $x_I^{(T)}$ as the x_I – coordinate of a cross-section in the aft part of the ship where separation occurs. Skejic (2008) proposes choosing $x_I^{(T)}$ at a position just ahead of the propeller plane.

If the two ships are in the far-field of each other, have parallel course and no transverse and yaw angular velocities, we may apply the Tuck and Newman's (1974) slender-body theory for hull interaction to find expressions for the lift force and moment acting on the ships. It seems possible to generalize this theory to consider two ships on a general course relative to each other and assuming that the two ships are in the far-field of each other. The effect of transverse and yaw ship velocities have a dipole-like behavior in the far-field while the forward speed implies that the bow and stern will separately have a source-like and sink-like effect, respectively. Because a source/sink behavior is more dominant in the far-field than a dipole-like behavior, it suggests that the dominant interaction effects between two ships are due to their forward speeds as long as they are not too close.

Viscous hull loads due to cross-flow separation

Viscous hull loads due to cross-flow separation may be incorporated by means of empirical drag coefficients. One ought to account for the fact that the cross-flow separation is more pronounced in the aft part than in the forward part of a ship advancing with a forward speed. The latter fact can, for instance, be understood by applying a *2D+t* method as shown in Faltinsen (2005). However, a *2D+t* method would require a 2D CFD method which becomes unpractical in terms of required CPU time in realistic maneuvering simulations. Further, it is not consistent to add together flow separation effects and potential flow effects without cross-flow separation. Formulation of viscous transverse force and yaw moment based on strip theory and the cross-flow principle is sometimes used but cannot adequately describe the effect of flow separation at realistic forward speeds and transverse ship velocities along the ship. If PMM tests are available with proper consideration of Reynolds-number effects, information about the global viscous loads due to flow separation can be provided. The cross-flow separation will also affect the longitudinal force. The latter fact is common to account for in the analysis of a single ship in water of infinite horizontal extent. The longitudinal non-lifting hull force can then according to eq. (8) be expressed as $X_{NLH}^{(1)} = -A_{11}\dot{u}_1 + u_3\left(A_{22}u_2 + A_{23}u_3\right)$. The nonlinear term $A_{22}u_3u_2$ can cause important longitudinal drag and it is common to modify the term as $C_{TN}A_{22}u_3u_2$ where C_{TN} is a hull-dependent empirical reduction coefficient due to cross-flow separation. The nonlinear viscous loads associated with cross-flow separation have an important role in simulating a tight circular maneuver. We are in our simulation studies neglecting the viscous cross-flow separation effect due to the fact that the radiuses of curvature of the vessels paths are sufficiently large.

Ship resistance

Hull resistance based on standard formulations for a ship on a straight course with constant speed (see e.g. Faltinsen, 2005) is incorporated in the maneuvering model. The ITTC 1957 model-ship correlation line is used to calculate the friction coefficient C_F for a smooth hull surface. The expression for the hull form factor k is based on regression analysis of experimental results (Skejic, 2008). A frictional force correction that accounts for correlation between model tests and full scale and includes the effect of surface roughness is added. The wave-making resistance R_W is a small part of the total resistance since the Froude number for maneuvers involving ship-ship interaction are generally small. As an option it is predicted by a 3D Rankine source method.

Propulsion and rudder loads

The propeller thrust is estimated as in Lewandowski (2004) and Skejic (2008). It means that the thrust-deduction coefficient t and the wake factor w are determined using Holtrop's regression formulas. The thrust coefficient is based on Wageningen B-series data and by regression analysis expressed as a cubic function of the advance ratio. The control system will adjust the thrust by changing the propeller revolutions n per second according to the propulsion controller.

The hydrodynamic drag, lift and yaw moment due to the rudder follow the descriptions in Faltinsen (2005) and Skejic (2008). Both the transverse ship velocity at the rudder and the rudder angle contributes to the angle of attack of the rudder. An effective longitudinal incident flow velocity to the rudders account for the increased axial slip stream velocity from the propeller.

Control system modeling

The control system (autopilot) is modeled following the procedures of Skejic (2008) and Skejic et al. (2009) for overtaking and lightering operations. The present study adopts identical control laws for the purpose of comparison and verification. The lightering maneuver is realized via a heading controller combined with a propulsion controller. Skejic et al. (2009) implemented such a controller for the simulation of a lightering system. The application of present maneuvering model follows the same procedures as detailed in Skejic et al. (2009), for which the main function is described as the autopilot always tries to reach specified (a) transverse distance *e*; (b) longitudinal distance *s*; (c) heading angle ψ_d; (d) relative speed between two ships in operation. The autopilot uses the required transverse distance *e* as input to the steering/heading control module, while at the same time the propulsion/speed control model uses the required longitudinal distance as the input for longitudinal alignment. A PD and a PI controller are applied for the heading and speed control respectively. The only difference of the present overtaking maneuver from a lightering maneuver in Skejic et al. (2009) is that the side-by-side offloading scenario is neglected, which means that both the heading/clearance controller and speed controller are implemented during the simulation.

Verification and validation

The added mass terms in the present maneuvering model are time-varying. For verification, we study the added masses of two identical interacting spheres at different relative positions that are moving towards each other with the same velocity. The x_I-axes are in the opposite direction. The centers of sphere 1 and 2 have coordinates $(0,0,0)$ and $(x,0,0)$ in the $O_1x_1y_1z_1-$coordinate system. Computed values of $A_{11}=A_{44}$ and $A_{14}=A_{41}$ have been verified by comparing with analytical results by Lamb (1932) as a function of x/R where R is the radius of the spheres. Results are presented in Fig. 2 in terms of the difference relative to the added mass $A_{11}=2\rho\pi R^3/3$ of a single sphere in infinite fluid. The hydrodynamic interaction almost vanishes when the two spheres are 4 times the diameter away from each other. The force associated with the added mass terms along the x_1-axis on body 1 can be expressed as

$$-\frac{d\left[\left(A_{11}+A_{14}\right)ds/dt\right]}{dt}=-\frac{d\left(A_{11}+A_{14}\right)}{ds}\left(\frac{ds}{dt}\right)^2-\left(A_{11}+A_{14}\right)\frac{d^2s}{dt^2} \quad (17)$$

where $ds/dt=u_1=u_4$. We imagine a wall perpendicular to the x_1-axis and midways between the two centers of the spheres. The interpretation of the last term is that $A_{11}+A_{14}$ is the added mass of a sphere next to the wall in a mode perpendicular to the wall. We see from the presented results in Fig. 2 that the largest influence from the wall is through the $A_{14}-$term. If ds/dt is constant, eq. (17) results in a force term that repulses the sphere from the wall. If the wall S_W is used as a control surface in eq. (15), it becomes clear that the remaining force part $0.5\rho\iint_{S_W}\mathbf{V}\cdot\mathbf{V}dS$ along the x_1-axis is positive.

We consider now two axis-symmetric bodies with pointed ends in infinite fluid advancing parallel to each other with steady forward speed along the x_I-axis which are also the symmetry axes for the bodies.

The body surfaces are defined by the x_I-dependent radius $r_I(x_I)=R_I\left[1-(x_I/L_I)^2\right]$ for $|x_I|\le L_I$ where $R_I\,(I=1,2)$ are the maximum radius of the bodies and $2L_I$ are the body lengths. The considered bodies are slender and the slenderness parameter is defined as $\varepsilon=R_I/(2L_I)$. We define x and $2p$ as the longitudinal and transverse distances between the two body centers.

The first case examines two identical axis-symmetric bodies with no stagger $(x=0)$ that advance with the same constant speed $u_1=u_4$. The slenderness parameter $\varepsilon=0.05$. Because the bodies have pointed ends, there is no lifting effect. We consider the transverse force $Y^{(1)}_{NLH}$ expressed by eq. (9). The contribution to the force comes from the term with a surface integral over the wetted hull surface $S^{(1)}_H$ which expresses the fact that there is a suction force between the two bodies. Our predictions are compared with the analytical results from Tuck and Newman

(1974) and Wang (2007) based on far-field and near-field slender body theory (SBT) respectively, and the 3D BEM results from the commercial software VSAERO (AMI) (Wang, 2007) in Fig. 3. The non-dimensional transverse force $Y^{(1)}_{NLH} / \left[\rho u_1^2 (2L_1)^2 \varepsilon^3\right]$ on body 1 is presented as function of non-dimensional transverse distance p / R_1 between the two body axes. The figure shows that the present BEM result agrees well with the VSAERO (AMI) result. There is satisfactory agreement with the far-field and near-field results when p / R_1 is larger than 6 and less than 3, respectively.

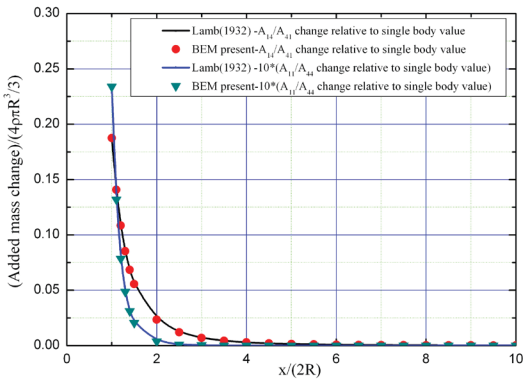

Fig. 2: Added mass change relative to single body value of two approaching identical spheres; shown comparison includes the A_{11} and A_{44} induced by the surge mode of each sphere on itself and A_{14} and A_{41} induced by the surge mode of the other

In the second case we study the same two axis-symmetric bodies as defined above. However, we let body 1 be stationary (moored) and let body 2 advance with constant speed u_4. The non-dimensional transverse distance between the two bodies are $p / R_1 = 6$. The non-dimensional transverse force $Y^{(1)}_{NLH} / \left[\rho u_4^2 (2L_1)^2 \varepsilon^3\right]$ and yaw moment $N^{(1)}_{NLH} / \left[\rho u_4^2 (2L_1)^2 \varepsilon^3\right]$ are presented as a function of the non-dimensional stagger x / L_1 in Fig. 4. Our results are compared with the far-field slender body theory by Tuck and Newman (1974). There is good agreement between the methods which should also be anticipated from Fig. 3 due to the fact that p / R_1 is sufficiently large. The peak sway force predicted by the Tuck - Newman method is slightly lower than the BEM, which is consistent with the results in Fig. 3.

The yaw moment predicted by the two approaches is almost indistinguishable. Starting from that ship 2 is far astern of ship 1; the transverse force acting on the two ships becomes first a repulsion force as a function of decreasing stagger until it becomes a suction force. The maximum suction force is when the ships have no stagger. The absolute value of the repulsion force is largest when the center of the passing ship is at the longitudinal position of the stern of the moored ship. Increasing the stagger with ship 2 ahead of ship 1 will finally cause a repulsion force again. The yaw moment is zero when the ships have no stagger and is negative when ship 2 is astern of ship 1 while it is positive when ship 2 is ahead of the moored ship. Positive yaw moment implies in a quasi-steady analysis that the bow of the moored ship moves towards the passing ship. The largest absolute values of the yaw moment on the moored ship are when the center of the passing ship is either ~ 0.15 times the ship length ahead or astern of the center of the moored ship. The time derivative terms in the force and moment expression are important in explaining the load behavior.

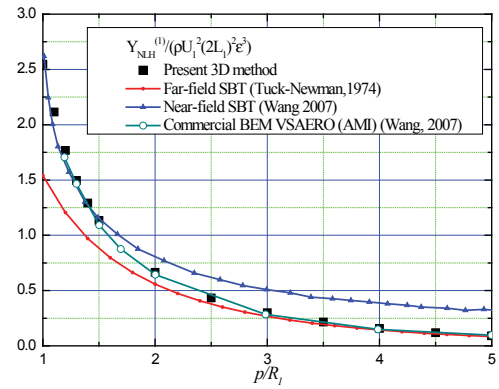

Fig. 3: Lateral force $Y^{(1)}_{NLH}$ acting on one of two identical axis-symmetric bodies with no stagger advancing with constant forward speed u_1=u_4 versus non-dimensional lateral distance between the body axes. The slenderness parameter ε=0.05. Calculated values by present 3D method, the BEM by VSAERO (AMI) (Wang, 2007), far-field slender body theory of Tuck and Newman (1974) and the near-field results of Wang (2007)

Our method is also compared with the sway interaction force from model tests presented by De Decker (2006) for two oil tankers; see Table 1 for main particulars and Fig. 5 for results. The lateral distance between centerlines of the two tankers is 1.2 times the average beam and the longitudinal distance between mid-sections vary from -0.5 to 0.5 times the average ship length. During each towing run the two

ships are fixed relative to each other and the transverse force is measured for ship 1. The prediction shows good agreement with the model test, especially near the force peak. The details and more results from the model tests are given by De Decker (2006).

Table 1: Main particulars for the MARINTEK model tests

Items	Ship 1 (full scale)	Ship 2(full scale)
L_{pp} (m)	317.7	226.4
Beam/B (m)	57.3	38.6
Draft/D (m)	20.0	7.5
Displacement (m^3)	289 068	51 974
Block coefficient/ C_B	0.792	0.794

A practical consideration is the computation time for a real-time simulation applying the current model. The BEM solver is dominating in time-cost. However, we do not need to run the solver every time step. This is because the interaction effects vanish fast with the relative distance between ships. In practice, the BEM solver can be run once at the beginning and then re-started when the longitudinal distance between two ships is less than 2.5 times the average ships' length.

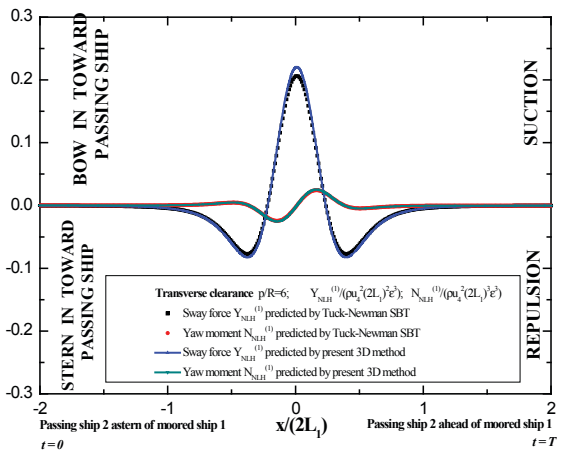

Fig. 4: Calm-water results for the interaction sway force and yaw moment on the moored slender body 1 due to passage of an identical slender body 2

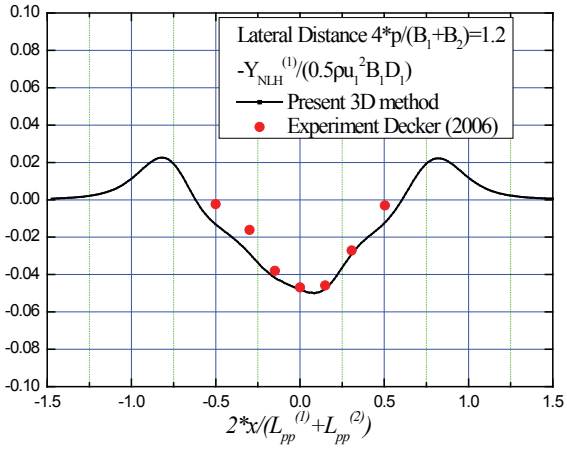

Fig. 7: Comparison of predicted transverse interaction force between two oil tankers with De Decker's experimental results at Marintek (2006)

Application: MARINER overtaking a scaled MARINER

The presented maneuvering model is applied in combination with the previously described autopilot model for one MARINER passing a 1.4 times scaled MARINER. The ship length and beam of the MARINER is L_{pp}=160.934m and B=23.165m, respectively. The case is identical to that by Skejic (2008). Details about the ships and maneuvering scenario can be found in Skejic (2008). The starting positions in the global coordinate system of the overtaken ship 1 and overtaking ship 2 are (0, 0) and (-1200m, -57.789m), respectively. The advancing speed is 10.5 knots for the overtaking ship and 8 knots for the overtaken. The desired lateral clearance between the centerlines of two ships is 30m+ (B_1+B_2)/2where the ship beams are B_1 *(I=1, 2)*. During the overtaking the autopilot is always trying to compensate the lateral clearance error via the rudder command. Thus collision can be avoided if the transverse clearance between two ships is not too small. It should be noted that in the present study a propulsion control is also applied. This is different from the study by Skejic (2008). The reason is that there is a longitudinal interaction force component in the present maneuvering model while Skejic (2008) does not account for this fact. Fig. 8 through Fig. 10 presents the comparison of present simulation of rudder control, lateral force and yaw moment with the identical case studied by Skejic (2008). . Fig. 11 shows the target and realized clearance between hull sides by the present controller, and Fig. 12 shows the realized speeds for the two ships. The results

qualitatively agree with each other. The current simulation gives higher value for the force/moment and rudder command. This is caused by the different hydrodynamic solvers used for the interaction effects between the two ships. Generally speaking, the Tuck-Newman far-field slender-body theory applied by Skejic (2008) tends to under-estimate the interaction effects when two ships are not sufficiently far away from each other (see Fig. 3). The overtaking case studied here uses a transverse clearance which is around 2 times the average beam and Fig. 3 shows that the 3D prediction will be around 20% higher than the Tuck-Newman theory for the sway force on the slender bodies used.

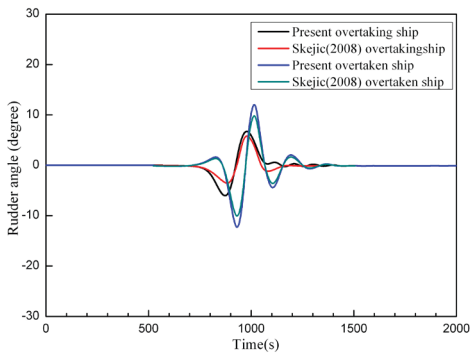

Fig. 8: Rudder control history of overtaking maneuver; overtaking ship 2: MARINER, overtaken ship 1: 1.4 times scaled MARINER. Starting position ship 2(-1200m, -57.789m), ship 1(0m, 0m) : compared with Skejic (2008)

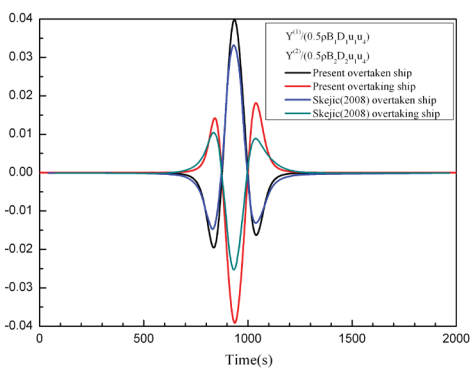

Fig. 9: Lateral force history of overtaking maneuver; overtaking ship 2: MARINER, overtaken ship 1: 1.4 times scaled MARINER: compared with Skejic (2008)

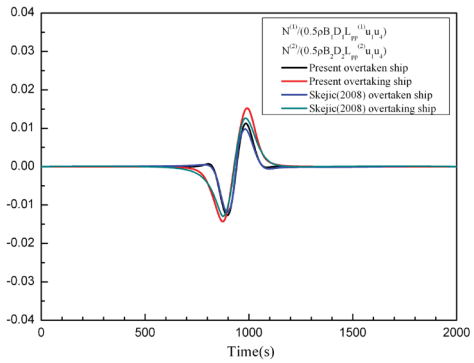

Fig. 10: Yaw moment history of overtaking maneuver; overtaking ship 2: MARINER, overtaken ship 1: 1.4 times scaled MARINER : compared with Skejic (2008)

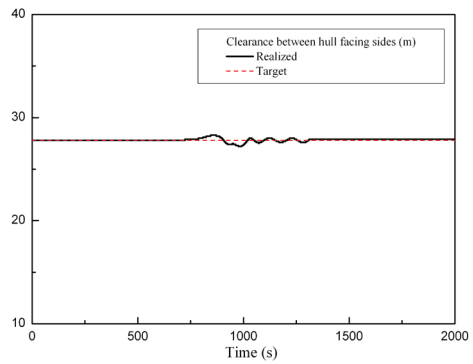

Fig. 11: Realized and target clearance between the two ships' facing sides by the present autopilot

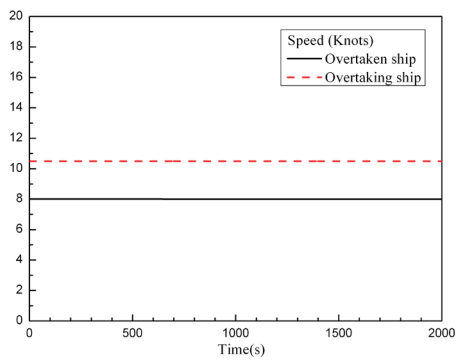

Fig. 12: Forward speed history of overtaking maneuver; overtaking ship 2: MARINER, overtaken ship 1: 1.4 times scaled MARINER

Concluding remarks

The maneuvering of two interacting ships in calm water at Froude numbers less than ~ 0.2 is studied based on an extended version of the maneuvering model for two ships by Skejic (2008). The time-varying interaction forces/moments and maneuvering hydrodynamic derivatives are obtained via a new method assuming 3D potential flow with rigid-free-surface condition around non-lifting bodies. The two bodies can have any relative positions and move with any velocities in the horizontal plane. It implies, for instance, that the method can be used up to the time of collision between two ships. The method is verified and validated for infinite fluid as well as water of infinite depth and infinite horizontal extent. The limitation of the far-field method by Tuck and Newman (1974) for two ships advancing with parallel courses with regard to separation distance between the ships is discussed. The proposed method is applicable for finite depth and can be generalized to more than two bodies and include channel effects.

Predictions of propulsion forces, rudder loads, viscous and lifting hull loads as well as the effect of an autopilot are implemented in order to make realistic maneuvering simulations. The maneuvering model is applied to an overtaking maneuver studied by Skejic (2008) showing that it matters to use the more complete interaction model instead of the far-field method by Tuck and Newman (1974).

How to include the effect of sea waves in terms of mean and slowly varying yaw moments and horizontal forces needs further studies. Practical simulations need also to account for wind and current.

Acknowledgement

The present work is funded by the Norwegian Research Council through CeSOS. Professor Tor E. Berg and Dr. Renato Skejic of MARINTEK have provided technical inputs of model test results, ship offsets and guidance.

References

Alvestad, R, and Brown, SH (1975). "Hybrid Computer Simulation of Maneuvering During Underway Replenishment in Calm and Regular Seas", International Shipbuilding Progress, 22, 250.

Cheng, L (2006). "Hydrodynamic interaction between two bodies", Doctoral thesis, School of shipbuilding, Harbin Engineering University, Harbin, China.

Cheng, L (2007). "Hydrodynamic interaction between two bodies", Journal of Hydrodynamics, Ser. B, 19, 6, pp. 784-785

De Decker, B (2006). "Ship-Ship Interaction during Lightering Operations", M.Sc. thesis, Marine Technology Department, Faculty of Marine Engineering, Gent, Belgium.

Faltinsen, OM (2005). "Hydrodynamics of High-Speed Marine Vehicles", New York: Cambridge University Press.

Ishiguro, T, Uchida, K, Manabe, T, Michida, R (1993). "A study on the maneuverability of the Super Slender Twin Hull", In Proc. FAST'93, ed. K. Sugai, H. Miyata, S. Kubo, H. Yamata, Vol. 1, pp. 283-94, Tokyo: The Society of Naval Architects of Japan.

Kochin, NE, Kibel, IA, Roze, NV, (1964). "Theoretical Hydromechanics", New York: Interscience Publishers.

Korsmeyer, FT, Lee, CH, and Newman, JN (1993). "Computation of ship interaction forces in restricted water". Journal of Ship Research,**37,** 4, pp. 298–306.

Lamb H (1932). Hydrodynamics, Dover Publications.

Lewandowski, Edward M (2004). "The Dynamics of Marine Craft". World Scientific.

Newman, JN. (1965). "The force and moment on a slender body of revolution moving near a wall", David Taylor Model Basin, Rep. 2127, Hydromechanics Laboratory, Washington D.C.,USA.

Newman, JN (1977). "Marine Hydrodynamics", MIT Press, Cambridge, MA.

Pinkster, JA (2004). "The influence of a free surface on passing ship effects", International Shipbuilding Progress, 51, 4 , pp. 313-338

Skejic, R. and Faltinsen, OM (2008). "A unified seakeeping and maneuvering analysis of ships in regular waves", J. of Marine Science and Technology.

Skejic, R (2008). "Maneuvering and Seakeeping of a Single Ship and of Two Ships in Interaction", Doctoral thesis, Department of Marine Technology, Faculty of Engineering Science and Technology, Norwegian University of Science and Technology, Trondheim, Norway.

Skejic, R, Breivik, M, Fossen, TI, Faltinsen, OM(2009). “Modeling and Control of Underway Replenishment Operations in Calm Water” 8th IFAC International Conference on Manoeuvring and Control of Marine Craft, Guarujá (SP), Brazil.

Søding, H (1982). Prediction of ship steering capabilities, Schiffstechnik, 29, pp. 3-29

Tuck, EO and Newman, JN (1974). "Hydrodynamic interaction between ships", Proc. of the 10th Symp. on Naval Hyd., Cambridge, Mass., USA, pp. 35–70.

Wang, QX (2007). "An analytical solution for two slender bodies of revolution translating in very close proximity", Journal of Fluid Mechanics, 582, pp. 223-251.

Yasukawa, H (2003). “Simulation of ship collision caused by hydrodynamic interaction between ships”, MARSIM’03, Kanazawa, Japan.